PHYSICAL REVIEW B **77**, 041409(R) (2008)

Interplay of Coulomb and electron-phonon interactions in graphene

D. M. Basko[1,*] and I. L. Aleiner[2]
[1]*International School of Advanced Studies (SISSA), via Beirut 2-4, 34014 Trieste, Italy*
[2]*Physics Department, Columbia University, New York, New York 10027, USA*
(Received 26 October 2007; published 18 January 2008)

We consider the mutual effect of the electron-phonon and strong Coulomb interactions on each other by summing up leading logarithmic corrections via the renormalization group approach. We find that the Coulomb interaction enhances electron coupling to the intervalley A_1 optical phonons, but not to the intravalley E_2 phonons.

DOI: 10.1103/PhysRevB.77.041409 PACS number(s): 73.23.−b, 71.38.−k, 73.50.Bk, 78.20.Bh

Electron-phonon coupling (EPC) in graphene is currently a subject of intense research. Experimental information on EPC is obtained by Raman spectroscopy[1–5] and angle-resolved photoemission spectroscopy.[6] Theoretically, EPC constants are usually calculated from density-functional theory (DFT),[7–9] where the exchange (Fock) term is treated in the local density approximation (LDA),[10] or the generalized gradient approximation (GGA).[11] Disagreement between the calculated EPC and the ARPES data has been pointed out in Ref. 8.

Also, the ratio between calculated EPC constants for different phonon modes disagrees with the ratio of the integrated intensities I_{D^*}/I_{G^*} of the corresponding two-phonon Raman peaks, as noted in Ref. 12. Namely, in the Raman spectrum of graphene, two two-phonon peaks are seen: the so-called D^* peak near $2\omega_{A_1}=2650\ \mathrm{cm}^{-1}$, and the G^* peak near $2\omega_{E_2}=3250\ \mathrm{cm}^{-1}$, corresponding to scalar A_1 phonons from the vicinity of the K point of the first Brillouin zone, and to pseudovector E_2 phonons from the vicinity of the Γ point, respectively. Experimentally, $I_{D^*}/I_{G^*}\approx 20$,[1] which cannot be reproduced with the EPC constants obtained from DFT calculations.

In this work we consider the mutual effect of weak electron-phonon and strong Coulomb interactions on each other by summing up leading logarithmic corrections via the renormalization group (RG) approach, which goes beyond the Hartree-Fock approximation. The Coulomb interaction is known to be a source of logarithmic renormalizations for Dirac fermions.[13–15] Coulomb renormalizations in graphene subject to a magnetic field have been considered in Ref. 16, and the Coulomb effect on static disorder in Refs. 17–19. To the best of our knowledge, Coulomb renormalization of EPC has never been considered; moreover, at energies higher than the phonon frequency, EPC itself is a source of logarithmic renormalizations, and has to be included in the RG procedure.

Upon solution of the RG equations, we obtain that (i) EPC tends to enhance Coulomb interaction, but not sufficiently to dominate over the flow to weak coupling, found earlier;[15] (ii) Coulomb interaction enhances the EPC only for the scalar A_1 phonons, while renormalization of the coupling to the pseudovector E_2 phonons is due only to EPC and is relatively weak, in agreement with the Raman data.[1]

We measure the single-electron energies from the Fermi level of undoped (half-filled) graphene. The Fermi surface of undoped graphene consists of two points, called K and K'. The graphene unit cell contains two atoms; each of them has one π orbital, so there are two electronic states for each point of the first Brillouin zone (we disregard the electron spin). Thus, there are exactly four electronic states with zero energy. An arbitrary linear combination of them is represented by a four-component column vector ψ. States with low energy are obtained by including a smooth position dependence $\psi(\mathbf{r})$, $\mathbf{r}\equiv(x,y)$. The low-energy Hamiltonian has the Dirac form[20] (hereinafter we imply the summation over the spin indices)

$$\hat{H}_{\mathrm{el}}=\int d^2\mathbf{r}\ \hat{\psi}^\dagger(\mathbf{r})(-iv\boldsymbol{\Sigma}\cdot\boldsymbol{\nabla})\hat{\psi}(\mathbf{r}). \tag{1}$$

We prefer not to give the explicit form of the isospin matrices $\boldsymbol{\Sigma}\equiv(\Sigma_x,\Sigma_y)$, which depends on the choice of basis (the specific arrangement of the components in the column ψ). We only note that all 16 generators of the SU(4) group, forming the basis in the space of 4×4 Hermitian matrices, can be classified according to the irreducible representations of C_{6v}, the point group of the graphene crystal (Tables I and II). They can be represented as products of two mutually commuting algebras of Pauli matrices $\Sigma_x,\Sigma_y,\Sigma_z$ and $\Lambda_x,\Lambda_y,\Lambda_z$,[21,22] which fixes their algebraic relations. By definition, Σ_x,Σ_y are the matrices, diagonal in the K,K' subspace, and transforming according to the E_1 representation of C_{6v}. The Fermi velocity $v\approx10^8$ cm/s.

The Hamiltonian of the long-range Coulomb interaction between electrons has the form

$$\hat{H}_{ee}=\frac{e^2}{2}\int d^2\mathbf{r}\,d^2\mathbf{r}'\frac{\hat{\rho}(\mathbf{r})\hat{\rho}(\mathbf{r}')}{|\mathbf{r}-\mathbf{r}'|},\quad \hat{\rho}(\mathbf{r})=\hat{\psi}^\dagger(\mathbf{r})\hat{\psi}(\mathbf{r}). \tag{2}$$

The background dielectric constant of the substrate is incorporated into e^2.

TABLE I. Irreducible representations of the group C_{6v} and their characters.

C_{6v}	E	C_2	$2C_3$	$2C_6$	$\sigma_{a,b,c}$	$\sigma'_{a,b,c}$
A_1	1	1	1	1	1	1
A_2	1	1	1	1	−1	−1
B_2	1	−1	1	−1	1	−1
B_1	1	−1	1	−1	−1	1
E_1	2	−2	−1	1	0	0
E_2	2	2	−1	−1	0	0

TABLE II. Classification of 4×4 Hermitian matrices by irreducible representations of the C_{6v} group. Matrices joined by braces transform through each other under translations. "Irrep" indicates an irreducible representation

Irrep	A_1	B_1	A_2	B_2	E_1	E_2
			Valley-diagonal matrices			
Matrix	$\mathbb{1}$	Λ_z	Σ_z	$\Lambda_z\Sigma_z$	Σ_x,Σ_y	$-\Lambda_z\Sigma_y,\Lambda_z\Sigma_x$
			Valley-off-diagonal matrices			
Matrix	$\overbrace{\Lambda_x\Sigma_z}$	$\overbrace{\Lambda_y\Sigma_z}$	$\overbrace{\Lambda_x}$	$\overbrace{\Lambda_y}$	$\overbrace{\Lambda_x\Sigma_y,-\Lambda_x\Sigma_x}$	$\overbrace{\Lambda_y\Sigma_x,\Lambda_y\Sigma_y}$

For low-energy electronic states EPC is efficient if the phonon wave vector is close to the Γ, K, or K' point. Considering only in-plane displacements, we have four degrees of freedom per unit cell. Consider the Γ point first. Two modes are acoustic; they weakly couple to electrons, and are neglected. The other two correspond to E_2 (pseudovector) optical phonons, shown in Fig. 1. They couple to the electronic motion via the KK'-diagonal E_2 matrices from Table II. The K and K' points are related by time-reversal symmetry, so the phonon frequencies are the same, and one can form real linear combinations of the modes from K and K'. They transform according to A_1, B_1, A_2, B_2, E_1, and E_2 representations of C_{6v}, and couple to the electronic motion via corresponding KK'-off-diagonal matrices. Linear coupling to A_2 and B_2 displacements is forbidden by time-reversal symmetry, and coupling to the E_1 and E_2 modes is numerically small.[23] The reason for this smallness is that E_1 and E_2 displacements do not change any C-C bond length; in the tight-binding approximation this coupling simply vanishes. Thus, we restrict our attention to the E_2 modes from the Γ point and A_1 and B_1 combinations of the modes from the K and K' points, shown in Fig. 1. They are the only modes seen in the Raman spectra of graphene.[1–5]

We take the magnitude of the carbon atom displacement as the normal coordinate for each mode, denoted by u_μ, $\mu=x,y,a,b$ for the four modes, shown in Fig. 1, respectively. Upon quantization of the phonon field, $\hat{u}_\mu$ and the phonon Hamiltonian $\hat{H}_{\rm ph}$ are expressed in terms of the creation and annihilation operators $\hat{b}^\dagger_{\mathbf{q}\mu}$ and $\hat{b}_{\mathbf{q}\mu}$ as

$$\hat{u}_\mu(\mathbf{r})=\sum_{\mathbf{q}}\frac{\hat{b}_{\mathbf{q}\mu}e^{i\mathbf{q}\cdot\mathbf{r}}+\text{H.c.}}{\sqrt{2NM\omega_\mu}},\quad \hat{H}_{\rm ph}=\sum_{\mathbf{q},\mu}\omega_\mu\hat{b}^\dagger_{\mathbf{q}\mu}\hat{b}_{\mathbf{q}\mu}. \tag{3}$$

The crystal is assumed to have the area L_xL_y, and to contain N carbon atoms of mass M. The $\mathbf{q}$ summation is performed

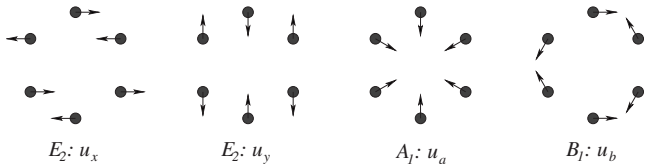

FIG. 1. Phonon displacements for E_2, A_1, and B_1 modes.

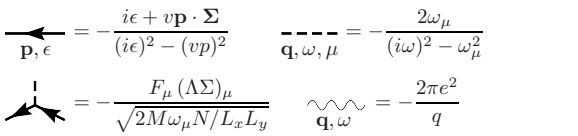

FIG. 2. Analytical expressions of the diagrammatic technique.

as $\Sigma_{\mathbf{q}}\to L_xL_y\int d^2\mathbf{q}/(2\pi)^2$. H.c. stands for the Hermitian conjugate. The two degenerate E_2 modes have the frequency $\omega_{E_2}\approx0.196$ eV. As the A_1 and B_1 modes represent real linear combinations of modes from the K and K' points, they have the same frequency $\omega_{A_1}\approx0.170$ eV, and appear with the same coupling constant in the EPC Hamiltonian:

$$\begin{aligned}\hat{H}_{\rm EPC}&=\int d^2\mathbf{r}\,\hat{\psi}^\dagger(\mathbf{r})\Big(\sum_\mu F_\mu\hat{u}_\mu(\mathbf{r})(\Lambda\Sigma)_\mu\Big)\hat{\psi}(\mathbf{r})\\&=\int d^2\mathbf{r}\,\hat{\psi}^\dagger(\mathbf{r})\{F_{E_2}[\hat{u}_x(\mathbf{r})\Lambda_z\Sigma_y-\hat{u}_y(\mathbf{r})\Lambda_z\Sigma_x]\\&\quad+F_{A_1}[\hat{u}_a(\mathbf{r})\Lambda_x\Sigma_z+\hat{u}_b(\mathbf{r})\Lambda_y\Sigma_z]\}\hat{\psi}(\mathbf{r}).\end{aligned} \tag{4}$$

The coupling constants F_{E_2} and F_{A_1} are not related by any symmetry. However, in the tight-binding model $F_{E_2}=F_{A_1}=3(\partial t_0/\partial a)$, where t_0 is the nearest-neighbor coupling matrix element, and a is the bond length.

As we are interested in energies much higher than the temperature T, we set $T=0$; still, calculations are much more transparent in the Matsubara representation. Electron and phonon Green's functions are given by

$$G(\mathbf{p},i\epsilon)=-\frac{i\epsilon+v\mathbf{p}\cdot\boldsymbol{\Sigma}}{\epsilon^2+(vp)^2},\quad D_\mu(i\omega)=-\frac{2\omega_\mu}{\omega^2+\omega_\mu^2}; \tag{5}$$

their graphical representation is shown in Fig. 2. The electronic self-energy is a sum of the Coulomb[15] and EPC (Ref. 24) contributions: $\Sigma=\Sigma^{ee}+\Sigma^{\rm ph}$, shown in Fig. 3.

The leading logarithmic term in Σ^{ee} is given by[15]

$$\begin{aligned}\Sigma^{ee}(\mathbf{p},i\epsilon)&=-\int\frac{d\omega}{2\pi}\frac{d^2\mathbf{q}}{(2\pi)^2}V(\mathbf{q},i\omega)G(\mathbf{p}-\mathbf{q},i\epsilon-i\omega)\\&\approx\frac{8}{\pi^2\mathcal{N}}[f(g)(2i\epsilon-v\mathbf{p}\cdot\boldsymbol{\Sigma})\\&\quad-\tilde{f}(g)(i\epsilon-v\mathbf{p}\cdot\boldsymbol{\Sigma})]\ln\frac{\xi_{\max}}{\xi_{\min}},\end{aligned} \tag{6}$$

$$f(g)=1-\frac{\pi}{2g}+\frac{\arccos g}{g\sqrt{1-g^2}},\quad \tilde{f}(g)=\frac{g\arccos g}{\sqrt{1-g^2}}, \tag{7}$$

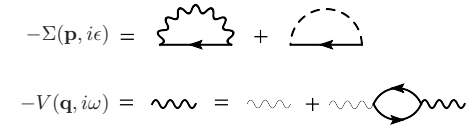

FIG. 3. Electron self-energy due to the screened Coulomb interaction and the EPC.

$$V(\mathbf{q},i\omega)=\frac{16g}{\mathcal{N}}\frac{v}{q}\frac{\sqrt{(vq)^2+\omega^2}}{gvq+\sqrt{(vq)^2+\omega^2}},\quad g=\frac{\pi\mathcal{N}e^2}{8v}. \tag{8}$$

$\mathcal{N}=4$ is the number of Dirac species, valley and spin degeneracy taken into account. The lower cutoff $\xi_{\min}\sim\max\{vp,\epsilon\}$; the upper cutoff $\xi_{\max}\sim v/a$ is of the order of the electronic bandwidth. The logarithmic divergence in the Fock self-energy Σ^{ee} is due to the long-distance nature of the Coulomb interaction, and thus is not picked up by local approximations such as the LDA or GGA. The random phase approximation (RPA) for $V(\mathbf{q},i\omega)$, shown in Fig. 3, corresponds to expansion of the prelogarithm coefficient to the leading order in the parameter $1/\mathcal{N}=0.25$, assumed to be small. This is justified better than expansion in the dimensionless coupling constant g, obtained with the bare coupling $2\pi e^2/q$. Indeed, for $\mathcal{N}=4$ we have $g=(\pi/2)(e^2/v)\approx 3.4$; background dielectric screening reduces it to $g\sim 1$.

The leading logarithmic asymptotics of Σ^{ph} is given by

$$\Sigma^{\mathrm{ph}}(i\epsilon)=-\int\frac{d\omega}{2\pi}\frac{d^2\mathbf{q}}{(2\pi)^2}\sum_\mu\frac{F_\mu^2}{2M\omega_\mu}\frac{\sqrt{27}a^2}{4}D_\mu(i\omega)\times(\Lambda\Sigma)_\mu G(\mathbf{p}-\mathbf{q},i\epsilon-i\omega)(\Lambda\Sigma)_\mu \approx\frac{\lambda_{E_2}+\lambda_{A_1}}{2\pi}i\epsilon\ln\frac{\xi_{\max}}{\xi_{\min}},\quad \lambda_\mu=\frac{F_\mu^2}{M\omega_\mu v^2}\frac{\sqrt{27}a^2}{4}. \tag{9}$$

Here $\xi_{\min}\sim\max\{\epsilon,\omega_\mu\}$, $\xi_{\max}\sim v/a$, and $\sqrt{27}a^2/4$ is the area per carbon atom. The dimensionless constants λ_{E_2} and λ_{A_1} will be treated as small parameters.

The latter statement deserves some discussion. In principle, one could proceed analogously to the Coulomb case: instead of doing the perturbative expansion in λ_μ, one could dress the bare phonon propagators by the appropriate polarization operators $\Pi(\mathbf{q},i\omega)$, corresponding to $1/\mathcal{N}$ expansion. Since $\Pi(\mathbf{q},i\omega)\propto q$ at $\omega\ll q\ll 1/a$,[25] the dressed phonon frequency would grow as $\sqrt{q}$, and Σ^{ph} would no longer diverge logarithmically. However, the inelastic x-ray scattering data for the phonon dispersion[26] show that the phonon dispersion is smaller than the phonon frequency itself. Thus, the renormalization of the phonon frequency remains small even at $q\sim 1/a$, so the perturbative expansion in λ_μ is more justified.

The logarithmically divergent integrals in Eqs. (6) and (9) have different structure due to different form of the screened interaction $V(\mathbf{q},i\omega)$ and the phonon propagator $D_\mu(i\omega)$. In Eq. (6) the integral is dominated by the frequencies $|\omega|\sim vq$, while in Eq. (9) it is $|\omega|\sim\omega_\mu$, since $D_\mu(i\omega)\propto 1/\omega^2$ at $|\omega|\gg\omega_\mu$. Thus, in the calculation of the leading logarithmic asymptotics it is sufficient to approximate $D_\mu(i\omega)\approx -2\pi\delta(\omega)$. This substitution makes the phonon propagator (combined with EPC vertices) formally analogous to the correlator of static disorder potential (i.e., from the point of view of electrons with $\epsilon\gg\omega_\mu$ the lattice is effectively frozen). Thus, renormalizations due to EPC at $\epsilon\gg\omega_\mu$ are equivalent to those due to static disorder.[17–19,22] This equivalence holds only in the leading order in EPC, since in higher orders the phonon propagator is dressed by polarization loops, and the static disorder correlator is not.

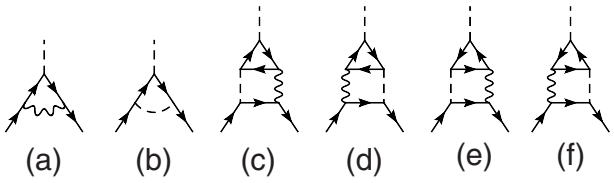

FIG. 4. Logarithmic corrections to the EPC vertex F_μ of the order $O(1/\mathcal{N},\lambda_\mu^2)$. Diagrams (c)–(f) vanish.

The presence of the large logarithm invalidates the first-order expansion in $1/\mathcal{N}$, and makes it necessary to sum all leading logarithmic terms $\sim(1/\mathcal{N})^n\ln^n$ of the perturbation theory. This is done using the standard RG procedure.[13–19] Let us introduce the running cutoff $\xi_{\max}e^{-\ell}$. One RG step consists of reducing the cutoff, $\ell\to\ell+\delta\ell$, so that $e^{-\delta\ell}\ll 1$, while $(1/\mathcal{N})\delta\ell\ll 1$, $\lambda_\mu\delta\ell\ll 1$. The inverse Green's function transforms as

$$i\epsilon-v\mathbf{p}\cdot\boldsymbol{\Sigma}-\Sigma(\mathbf{p},i\epsilon)=\frac{i\epsilon-(v+\delta v)\mathbf{p}\cdot\boldsymbol{\Sigma}}{1+\delta Z}, \tag{10}$$

where δZ is chosen to preserve the coefficient at $i\epsilon$ upon rescaling of the electronic fields, $\psi\to(1+\delta Z/2)\psi$: $\delta Z=\partial\Sigma(\mathbf{p},i\epsilon)/\partial(i\epsilon)$. Then v is renormalized as

$$\frac{\delta v}{v}=\frac{\partial\Sigma(\mathbf{p},i\epsilon)}{\partial(i\epsilon)}+\frac{\partial\Sigma(\mathbf{p},i\epsilon)}{\partial(v\mathbf{p}\cdot\boldsymbol{\Sigma})}. \tag{11}$$

Next, we determine renormalization of the coupling constants. The electron charge e is not changed, as guaranteed by the gauge invariance, so the renormalization of the Coulomb coupling constant g is determined by the velocity v. For the EPC, logarithmic vertex corrections of the order $O(1/\mathcal{N},\lambda_\mu^2)$ are shown in Fig. 4. Two other diagrams (Fig. 5) should be taken into account, as they are of the same order and also logarithmic. As a result, we obtain the following RG equations:

$$\frac{dg}{d\ell}=-\frac{8f(g)}{\pi^2\mathcal{N}}g+\frac{\lambda_{E_2}+\lambda_{A_1}}{2\pi}g, \tag{12a}$$

$$\frac{d\lambda_{E_2}}{d\ell}=\frac{\lambda_{A_1}^2}{2\pi}, \tag{12b}$$

$$\frac{d\lambda_{A_1}}{d\ell}=\frac{16f(g)}{\pi^2\mathcal{N}}\lambda_{A_1}. \tag{12c}$$

Because of the diagrams of Fig. 5, the renormalized λ_μ cannot be related to a new EPC vertex F_μ. Iterations of these

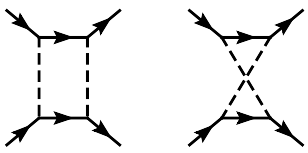

FIG. 5. Logarithmic diagrams of the order $O(\lambda_\mu^2)$ not reduced to a renormalization of the EPC vertex F_μ.

diagrams generate electron coupling to multiphonon excitations, all included in the renormalized λ_μ.

The coupling constant λ_{E_2} at energies $\sim\omega_{E_2}\approx 0.2$ eV can be extracted from the experimental data of Ref. 5 (change of the Raman G peak with the electron density): $\lambda_{E_2}\approx 0.035$, corresponding to $F_{E_2}=6$ eV/Å. Then the main effect comes from the Coulomb terms: as $f(g)>0$, g flows to weak coupling,[15] λ_{A_1} is enhanced, while the enhancement of λ_{E_2}, proportional to $\lambda_{A_1}^2$, is much weaker due to the cancellation between Coulomb self-energy and vertex corrections. This behavior is in qualitative agreement with the Raman data: when the λ_μ^2 term is neglected, the ratio of the intensities of the two-phonon peaks, mentioned in the introduction, is $I_D^*/I_G^*=2(\lambda_{A_1}/\lambda_{E_2})^2$.[12] If only Coulomb terms are kept in Eqs. (12), their integration gives $\lambda_{A_1}(\ell)/\lambda_{A_1}(0)=[g(0)/g(\ell)]^2=[v(\ell)/v(0)]^2$, which, in principle, can be checked experimentally.

To study the behavior of the coupling constants quantitatively, we solve Eqs. (12) numerically, neglecting the λ_μ^2 term. The largest value of ℓ is determined by the lower cutoff $\xi_{\min}\sim\omega_\mu\sim 0.2$ eV. In Fig. 6, we show the flow of λ_{A_1} for three values of the bare Coulomb coupling constant: $g(0)=3.4$ (corresponding to no dielectric screening at all), 1.5, and 0.5. The bare values of the electron-phonon coupling constants $\lambda_{E_2}(0)=0.035$, $\lambda_{A_1}(0)=0.040$ were chosen (a) to satisfy the relation $\lambda_{E_2}(0)/\lambda_{A_1}(0)=\omega_{A_1}/\omega_{E_2}$, valid in the tight-binding approximation, and (b) to reproduce the experimental value $\lambda_{E_2}\approx 0.035$. For electronic energies $\epsilon\sim 1$ eV, involved in the Raman scattering, in the totally unscreened case, $g(0)=3.4$, we obtain $\lambda_{A_1}/\lambda_{E_2}\approx 3.2$, in agreement with the observed ratio $I_D^*/I_G^*\approx 20$. Note that the RPA calculation without the RG collection of all leading logarithmic terms would give all dependencies in Fig. 6 to be straight lines with slopes fixed at 10 eV. A comparable error would be produced by the GW approximation, which neglects vertex corrections, and thus picks up correctly only the first term of the logarithmic series.

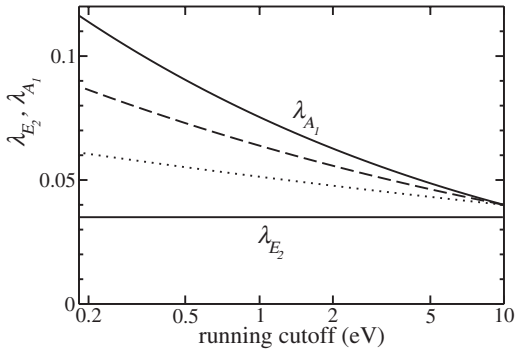

FIG. 6. Flow of the dimensionless coupling constants λ_{A_1} (three upper curves, starting from the bare value 0.04 at 10 eV) for three values of the bare Coulomb coupling $g(0)=3.4$, 1.5, and 0.5 (solid, dashed, and dotted curves). The constant $\lambda_{E_2}=0.035$ is unchanged in the order $O(\lambda)$.

To conclude, in this paper we have considered the mutual effect of the weak electron-phonon and strong Coulomb interactions on each other by summing up leading logarithmic corrections via the renormalization group approach in the intermediate energy range $\omega_{E_2},\omega_{A_1}<\epsilon<v/a$. At these energies quantum fluctuations of the phonon field may be viewed as effective static disorder. We find that Coulomb interaction enhances electron coupling to the intervalley A_1 optical phonons, but not to the intravalley E_2 phonons, in agreement with the experimental data for two-phonon Raman scattering.

We thank M. S. Foster, F. Guinea, and F. Mauri for helpful discussions.

*basko@sissa.it

[1] A. C. Ferrari *et al.*, Phys. Rev. Lett. **97**, 187401 (2006).
[2] A. Gupta *et al.*, Nano Lett. **6**, 2667 (2007).
[3] D. Graf *et al.*, Nano Lett. **7**, 238 (2007).
[4] S. Pisana *et al.*, Nat. Mater. **6**, 198 (2007).
[5] J. Yan, Y. Zhang, P. Kim, and A. Pinczuk, Phys. Rev. Lett. **98**, 166802 (2007).
[6] A. Bostwick *et al.*, Nat. Phys. **3**, 36 (2007).
[7] M. Lazzeri and F. Mauri, Phys. Rev. Lett. **97**, 266407 (2006).
[8] M. Calandra and F. Mauri, Phys. Rev. B **76**, 205411 (2007).
[9] C.-H. Park, F. Giustino, M. Cohen, and S. Louie, Phys. Rev. Lett. **99**, 086804 (2007).
[10] D. M. Ceperley and B. J. Alder, Phys. Rev. Lett. **45**, 566 (1980); J. P. Perdew and A. Zunger, Phys. Rev. B **23**, 5048 (1981).
[11] D. C. Langreth and M. J. Mehl, Phys. Rev. B **28**, 1809 (1983); A. D. Becke, Phys. Rev. A **38**, 3098 (1988); J. P. Perdew, K. Burke, and M. Ernzerhof, Phys. Rev. Lett. **77**, 3865 (1996).
[12] D. M. Basko, Phys. Rev. B **76**, 081405(R) (2007).
[13] A. A. Abrikosov and S. D. Beneslavskii, Zh. Eksp. Teor. Fiz. **59**, 1280 (1970) [Sov. Phys. JETP **32**, 699 (1971)].
[14] J. González, F. Guinea, and M. A. H. Vozmediano, Mod. Phys. Lett. B **7**, 1593 (1994); Nucl. Phys. B **424**, 595 (1994); J. Low Temp. Phys. **99**, 287 (1994).
[15] J. González, F. Guinea, and M. A. H. Vozmediano, Phys. Rev. B **59**, R2474 (1999).
[16] I. L. Aleiner, D. E. Kharzeev, and A. M. Tsvelik, Phys. Rev. B **76**, 195415 (2007).
[17] J. Ye, Phys. Rev. B **60**, 8290 (1999).
[18] T. Stauber, F. Guinea, and M. A. H. Vozmediano, Phys. Rev. B **71**, 041406(R) (2005).
[19] M. S. Foster and I. L. Aleiner (unpublished).
[20] P. R. Wallace, Phys. Rev. **71**, 622 (1947).
[21] E. McCann, K. Kechedzhi, V. I. Falko, H. Suzuura, T. Ando, and B. L. Altshuler, Phys. Rev. Lett. **97**, 146805 (2006).
[22] I. L. Aleiner and K. B. Efetov, Phys. Rev. Lett. **97**, 236801 (2006).
[23] S. Piscanec, M. Lazzeri, F. Mauri, A. C. Ferrari, and J. Robertson, Phys. Rev. Lett. **93**, 185503 (2004).
[24] Σ^{ph} in graphite was considered long ago [F. Guinea, J. Phys. C **14**, 3345 (1981)], but the logarithmic divergence was not noted in that work.
[25] Kenneth W.-K. Shung, Phys. Rev. B **34**, 979 (1986).
[26] J. Maultzsch, S. Reich, C. Thomsen, H. Requardt, and P. Ordejon, Phys. Rev. Lett. **92**, 075501 (2004).